

Electronic Supplementary Information

for

Solid-state polymerization in a polyrotaxane coordination polymer via [2+2] cycloaddition reaction

In-Hyeok Park,^a Raghavender Medishetty,^b Shim Sung Lee^{*a} and Jagadese J. Vittal^{*ab}

[†]Department of Chemistry and Research Institute of Natural Science, Gyeongsang National University, Jinju 660-701, S. Korea

[‡]Department of Chemistry, National University of Singapore, 3 Science Drive 3, Singapore 117543

TABLE OF CONTENTS

Experimental section. General and synthetic methods

X-ray crystallography. General and structural refinements for **1** and **2**

Table S1 Crystallographic data and refinement parameters for **1** and **2**

Fig. S1 Comparison of PXRD patterns for **1**

Fig. S2 Comparison of PXRD patterns for **2**

Fig. S3 TGA curve of **1**

Fig. S4 TGA curve of **2**

Fig. S5 A portion of the (4 × 4) grid in **1**

Fig. S6 Channel along *b*-axis in **1**

Fig. S7 The connectivity showing 2D polyrotaxane in **1**

Fig. S8 Disordered bpeb in **2**

Fig. S9 2-Fold interpenetrated 3D structure of **2**

Fig. S10 Topological representations of **2**

Fig. S11 The organic polymer *poly*-bppcb in **2**.

Fig. S12 ¹H NMR spectrum of **1**

Fig. S13 IR spectra of **1** and **2**

Experimental section

General. All chemicals were purchased of reagent grade and were used without further purification. The bpeb ligand was synthesized by the reported procedure.^{S1} The elemental analyses were carried out a LECO CHNS-932 elemental analyzer. The infrared spectra (IR) were recorded (4000 – 400 cm⁻¹) on the Thermo Fisher Scientific Nicolet iS 10 FT-IR spectrometer using KBr pellets. Thermogravimetric analyses (TGA) were performed under a nitrogen atmosphere with a heating rate of 5°C min⁻¹ using a TA Instruments TGA-Q50 thermogravimetric analyzer. The solid-state emission spectra were obtained from Shimadzu RF-5301PC. The NMR spectra were recorded with a Bruker DRX-500 with TMS as internal reference. For all the NMR spectra recorded, a drop of HNO₃ was added to dissolve the insoluble **1**. Powder X-ray diffraction (PXRD) patterns were recorded on a D8 DISCOVER with GADDS (Bruker AXS) with graphite monochromatized Cu-K α radiation ($\lambda = 1.54056 \text{ \AA}$) at room temperature (23°C).

[Cd(bpeb)(sdb)]·DMA (1): A mixture of bpeb (19.9 mg, 0.070 mmol), H₂sdb (21.7 mg, 0.071 mmol), and Cd(NO₃)₂·4H₂O (26.2 mg, 0.085 mmol) dissolved in DMA (3 mL), H₂O (1 mL), and DMSO (0.5 mL) were placed in a 10-mL glass tube, and then 3-4 drops of 0.1 M NaOH were added. The tube was sealed and kept at 100°C for 48 h, followed by cooling to room temperature over 8 h. Orange platy crystals suitable for X-ray analysis were obtained. The crystals were dried under vacuum for 6 h and characterized. (25.5 mg, Yield 34% based on Cd^{II} salt. ¹H-NMR (DMSO-*d*₆/HNO₃, 300 MHz, 298 K): $\delta = 8.87$ (*d*, 4H, Py-*H* of bpeb), 8.23 (*d*, 4H, Py-*H* of bpeb), 8.08-8.16 (*m*, 8H, Ph-*H* of sdb), 7.95 (*d*, 2H, CH=CH of bpeb), 7.88 (*s*, 4H, Ph-*H* of bpeb), 7.66 (*d*, 2H, CH=CH of bpeb). Anal. Calcd for [C₃₈H₃₃CdN₃O₇S]: C, 57.91; H, 4.22; N, 5.33. Found: C, 58.18; H, 3.76; N, 4.96%. IR (KBr pellet, cm⁻¹) 2924, 2853, 1604, 1355, 1296, 1159, 1101, 1026, 749 and 622. Solvent weight loss in TG, 5.9% (observed) and 5.8% (calculated).

[Cd(bpeb)_{0.5}(poly-bppcb)_{0.5}(sdb)]·DMA (2): Compound **2** was obtained by UV irradiation of single crystals of **1** for 48 h. The crystals for the characterization including the microanalysis were dried under vacuum for 6 h. Anal. Calcd for [Cd(bpeb)_{0.5}(poly-bppcb)_{0.5}(sdb)]·0.5DMA, [C₃₆H_{28.5}CdN_{2.5}O_{6.5}S]: C, 58.07; H, 3.86; N, 4.70. Found: C, 57.86; H, 3.81; N, 4.40%. IR (KBr pellet, cm⁻¹) 2925, 2854, 1606, 1406, 1295, 1229 (C-C bonds of cyclobutane), 1159, 1100, 1016, 749 and 622. Solvent weight loss in TG, 5.9% (observed) and 5.8% (calculated).

X-ray crystallography

General. Crystal data for **1** and **2** at -100°C were collected on a Bruker SMART APEX II ULTRA diffractometer equipped with graphite monochromated Mo K α radiation ($\lambda = 0.71073 \text{ \AA}$) generated by a rotating anode. Data collection, data reduction, and absorption correction were carried out using the software package of APEX2.^{S2} All of the calculations for the structure determination were carried out using the SHELXTL package.^{S3} Relevant crystal data collection and refinement data for the crystal structures of **1** and **2** are summarized in Table S1.

Structural refinements

Compound 1: Anisotropic thermal parameters were refined for all the non-hydrogen atoms in the main structure. The solvent region containing one DMA was found to be disordered. Ideal geometry was imposed with DFIX and SADI options and only the isotropic thermal parameter was refined for the non-hydrogen atoms of DMA. All the hydrogen atoms were added in calculated positions.

Compound 2: Total Potential Solvent Accessible Void Volume 356.0 \AA^3 (20.2%). One pyridyl and olefin groups (N1-C7) were disordered. Two models were included in the least-squares refinements with ideal geometries to these disordered groups. Only isotropic thermal parameters were refined to 0.55(1) and 0.45(1). Otherwise, the connectivity in the main structure is proven beyond any doubt. However, the solvent region was highly disordered as indicated by unreasonable thermal parameters and close contact indicated by CHECKCIF. This may be due to weakly diffracting nature as reflected from $R_{\text{int}} = 0.2035$ and only 2799 reflections ($>2\sigma(I)$) observed out of 6694 unique reflections. When we attempted to construct model in the solvent region (DMF), the refinement was completed with $R_1 = 0.1096$ and $wR_2 = 0.2747$ with 393 parameters and 2799 observations. Further solvent region has problem as highlighted by the CIF. Moreover, due to very low data/parameter ratio, the data were squeezed.^{S4} This model with the squeezed data has been found to be more acceptable.

References:

- S1. A. V. Gutov, E. B. Rusanov, L. V. Chepeleva, S. G. Garasevich, A. B. Ryabitskii and A. N. Chernega, *Russ. J. Gen. Chem.*, 2009, **79**, 1513–1518.
- S2. Bruker, APEX2 Version 2009.1-0 Data Collection and Processing Software; Bruker AXS Inc., Madison, Wisconsin, U.S.A., 2008.
- S3. Bruker, SHELXTL-PC Version 6.22 Program for Solution and Refinement of Crystal Structures; Bruker AXS Inc., Madison, Wisconsin, U.S.A. 2001.
- S4. A. L. Spek, *Acta Cryst.* 2009, **D65**, 148-155.

Table S1 Crystallographic data and refinement parameters for **1** and **2** (Squeezed data)

	1	2
formula	C ₃₈ H ₃₃ CdN ₃ O ₇ S	C ₃₄ H ₂₄ CdN ₂ O ₆ S
formula weight	788.13	701.01
crystal system	Triclinic	Triclinic
space group	<i>P</i> -1	<i>P</i> -1
<i>a</i> (Å)	7.3880(17)	7.4493(18)
<i>b</i> (Å)	15.153(4)	15.362(4)
<i>c</i> (Å)	15.551(3)	15.558(4)
α (deg)	91.805(14)	85.950(19)
β (deg)	95.361(14)	87.333(18)
γ (deg)	90.380(15)	82.947(18)
<i>V</i> (Å ³)	1732.4(7)	1761.3(7)
<i>Z</i>	2	2
<i>D</i> _{calc} (g/cm ³)	1.511	1.486
μ (mm ⁻¹)	0.745	0.733
$2\theta_{\max}$ (deg)	52.00	52.00
reflections collected	23581	19383
independent reflections	6741 [R(int) = 0.1168]	6694 [R(int) = 0.1701]
goodness-of-fit on <i>F</i> ²	1.005	0.922
<i>R</i> ₁ , <i>wR</i> ₂ [<i>I</i> > 2 σ (<i>I</i>)]	0.0866, 0.1411	0.0850, 0.1741
<i>R</i> ₁ , <i>wR</i> ₂ (all data)	0.2250, 0.2606	0.1858, 0.2023

CCDC 952014 & 952015 for **1** and **2** respectively.

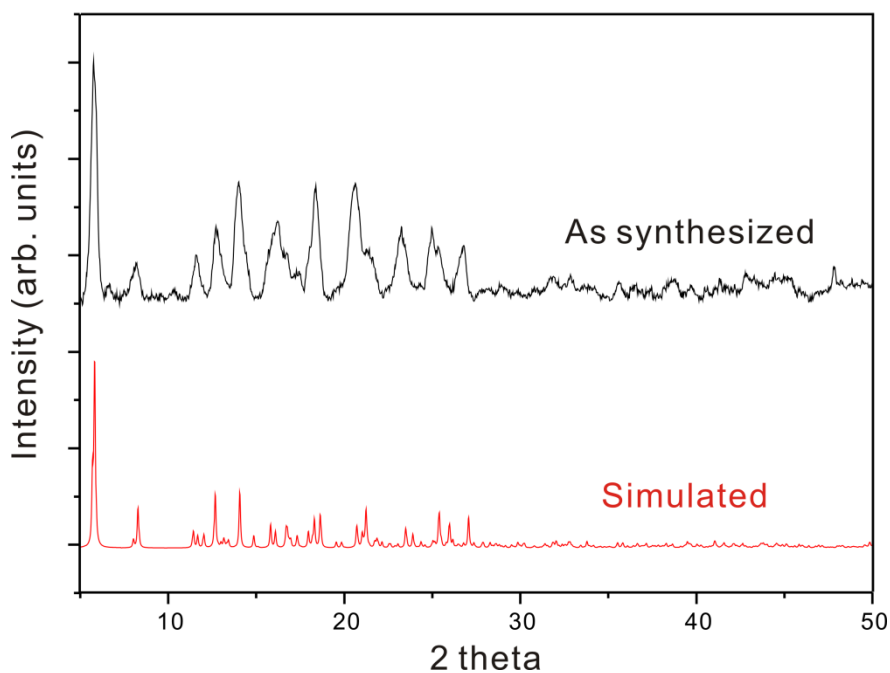


Fig. S1 PXRD patterns for **1**: (top) as synthesized and (bottom) simulated from the single crystal X-ray data. The intensity variations in these patterns may be due to the preferred orientations of the powder form or loss of solvents during grinding.

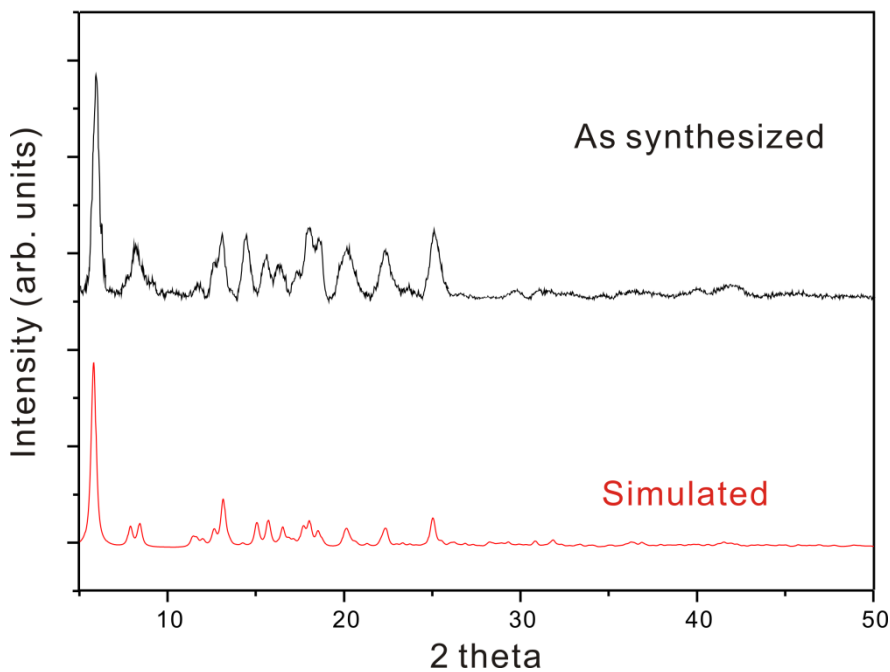


Fig. S2 PXRD patterns of **2**: (top) as synthesized and (bottom) simulated from the single crystal X-ray data. The intensity variations in these patterns appear to be due to the preferred orientations of the powder form or loss of solvents during grinding.

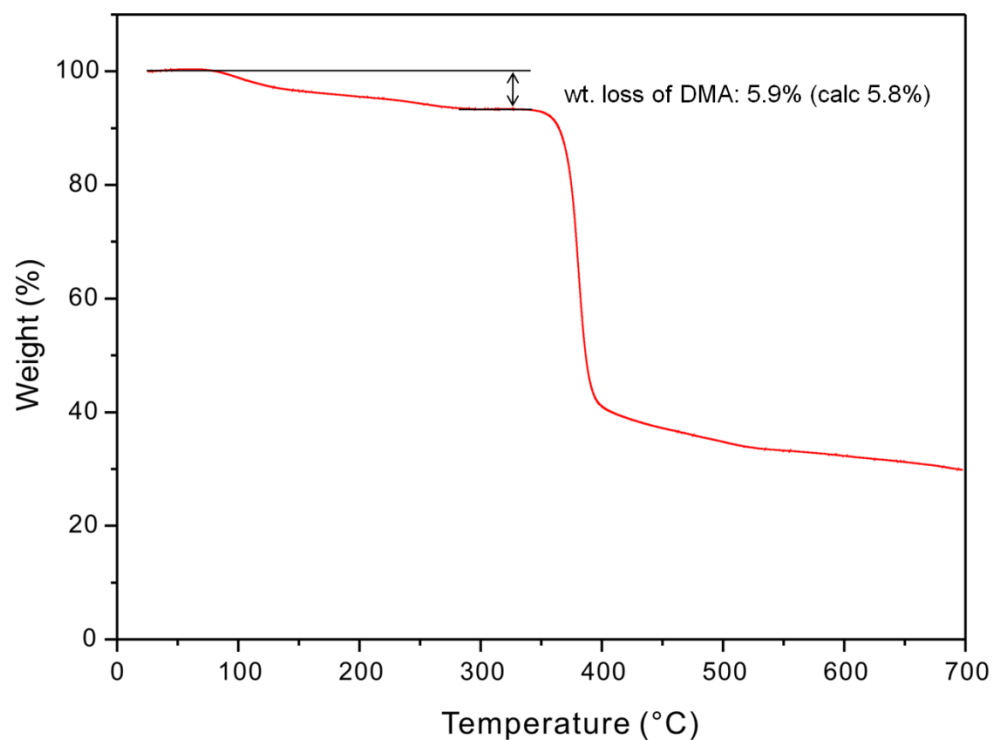


Fig. S3 TGA curve of **1** with heating rate of $5^{\circ}\text{C}\cdot\text{min}^{-1}$ under N_2 flow. The desolvated **1** is stable up to 350°C .

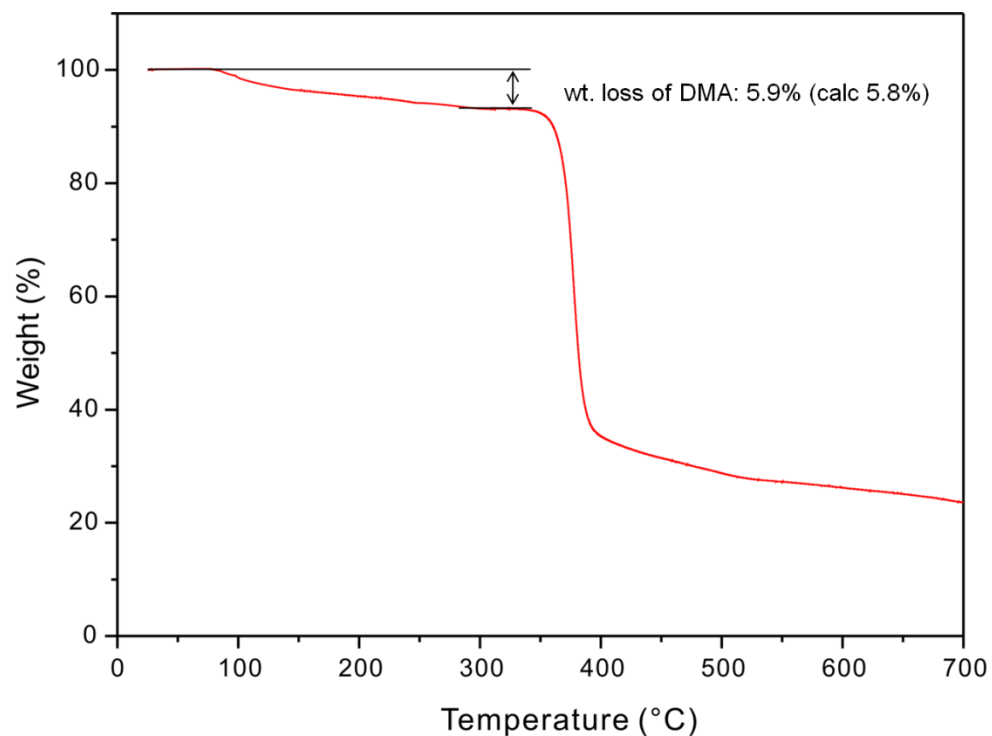


Fig. S4 TGA curve of **2** with heating rate of $5^{\circ}\text{C}\cdot\text{min}^{-1}$ under N_2 flow. The desolvated MOPF is stable up to 350°C .

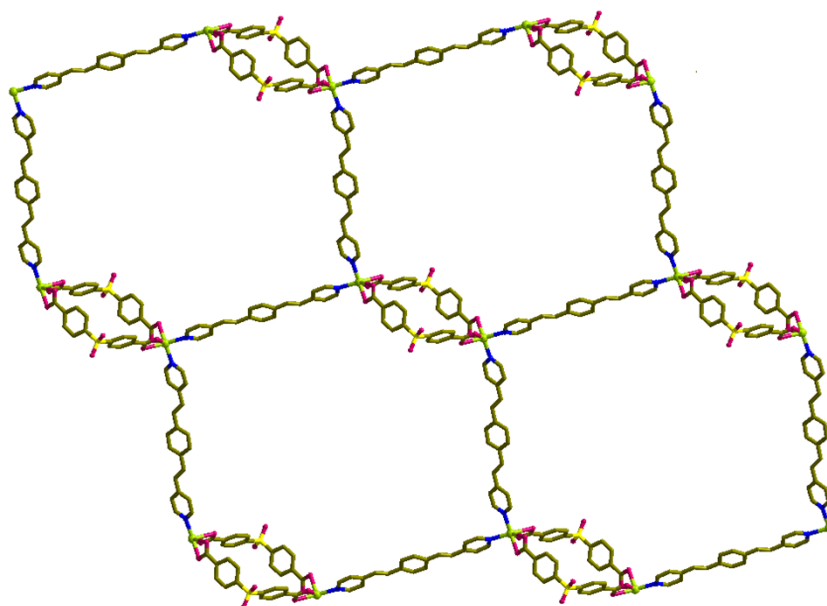


Fig. 5 A portion of the (4×4) grid in **1**.

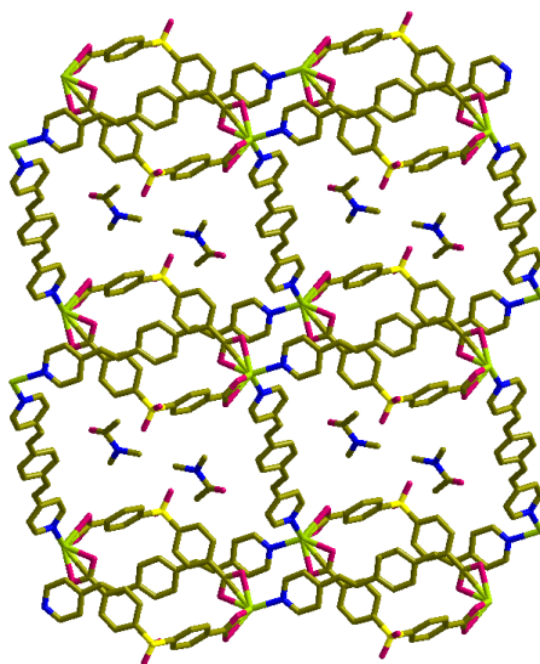


Fig. S6 DMA molecules are shown inside the channel viewed along a -axis in **1**.

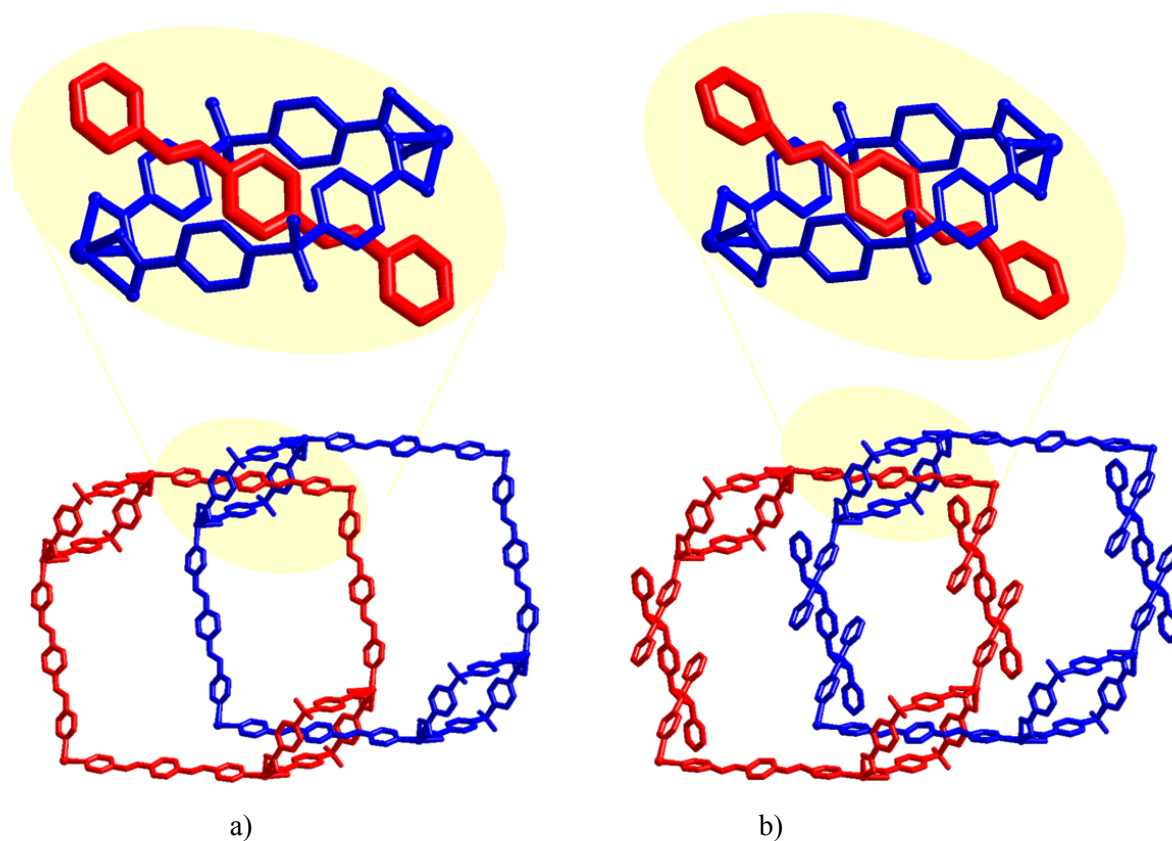


Fig. S7 The connectivity showing 2D polyrotaxane and blown-up section in (a) 1 and (b) 2.

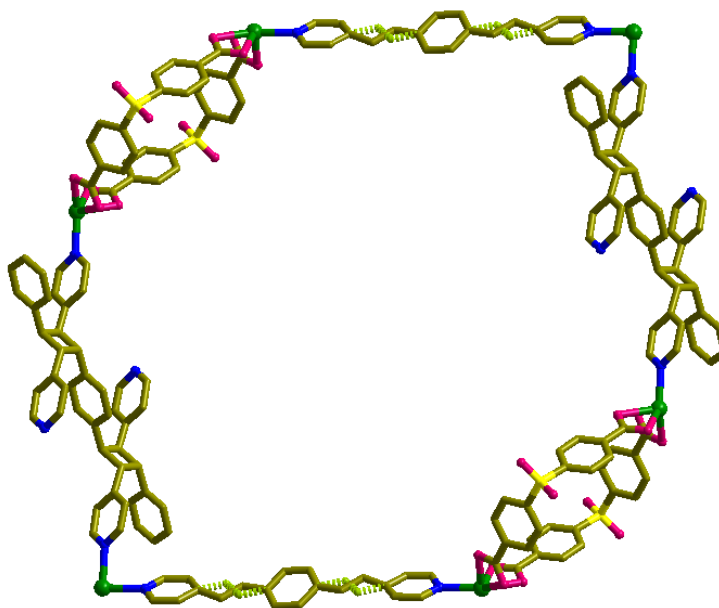


Fig. S8 A single net in 2 showing the disordered a conformation of the unreacted bpeb over two sites with occupancy ratio of approximately 55 : 45 (gold bond : dotted lime bond).

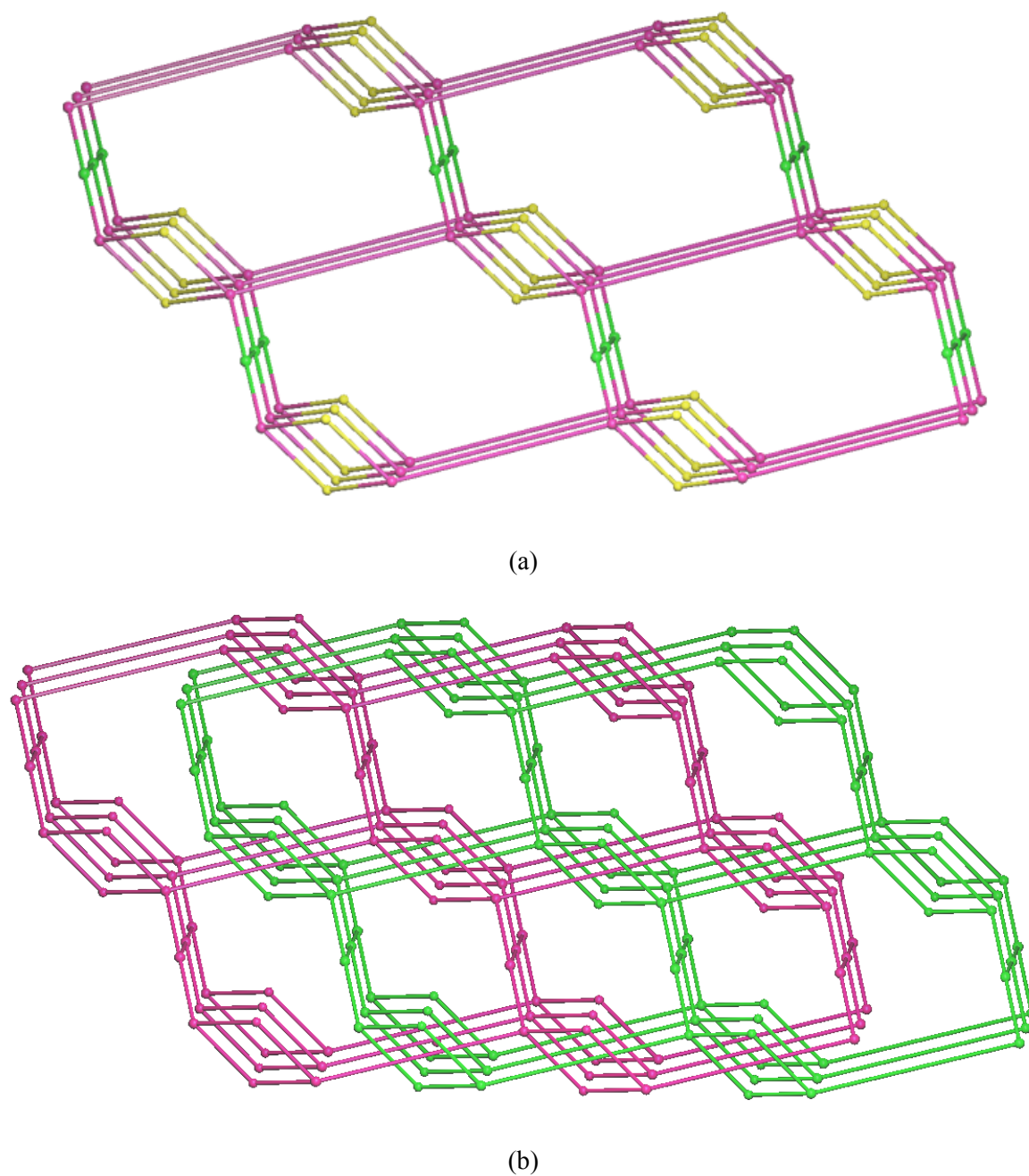


Fig. S9 (a) and (b) are schematic representations showing the connectivity without interpenetration and 2-fold interpenetrated 3D structure of **2**, respectively. Colour code: Cd node (pink), *poly*-bppcb node (green) and sulfur from sdc (yellow).

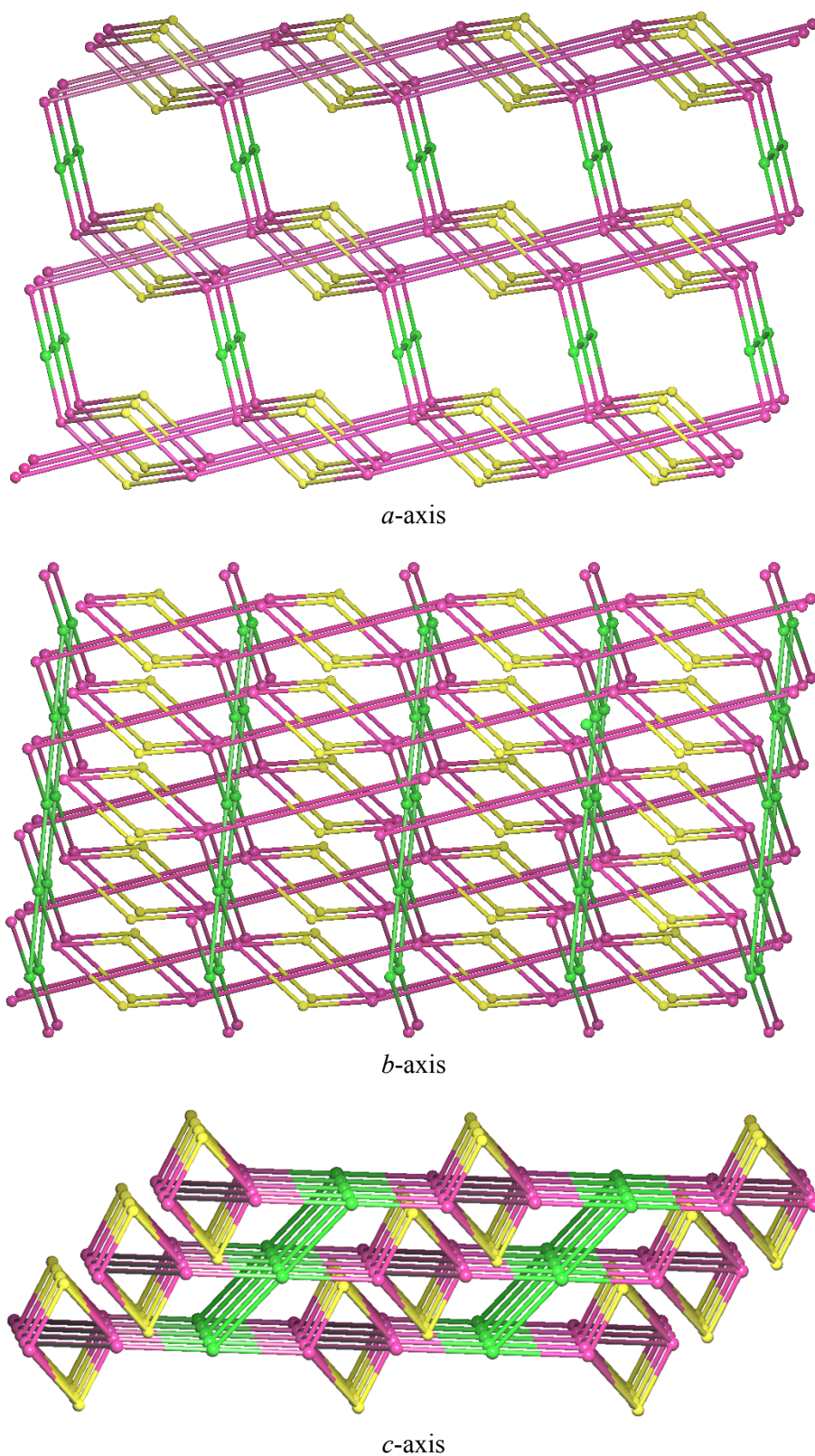


Fig. S10 Topological representations of the 2-interpenetrated 3D structures of **2** along the three principle axes. Colour code: Cd node (pink), *poly*-bppcb node (green) and sulfur from sdc (yellow).

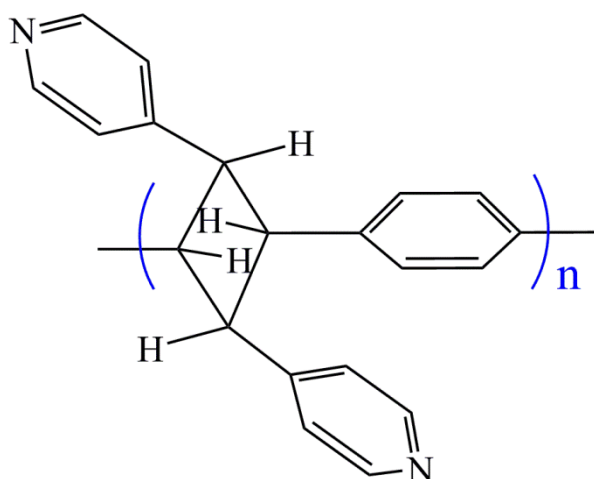


Fig. 11 The organic polymer *poly-bppcb* in **2**.

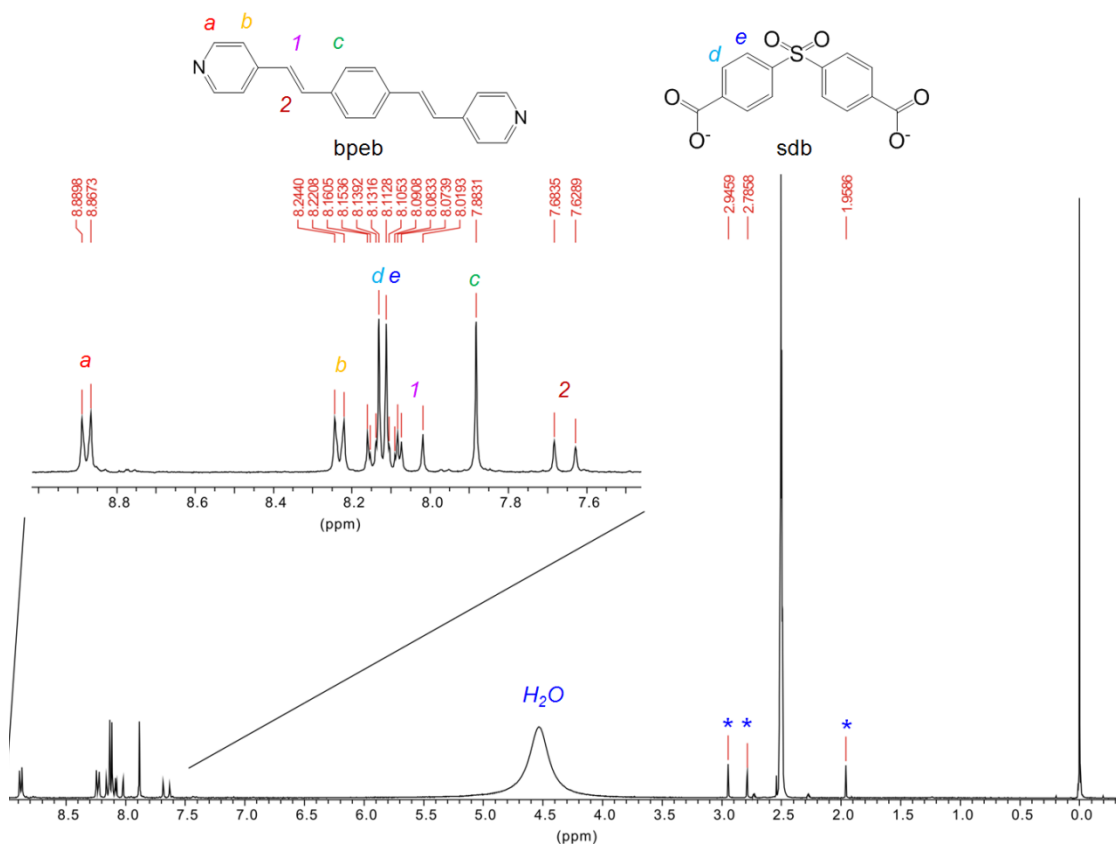
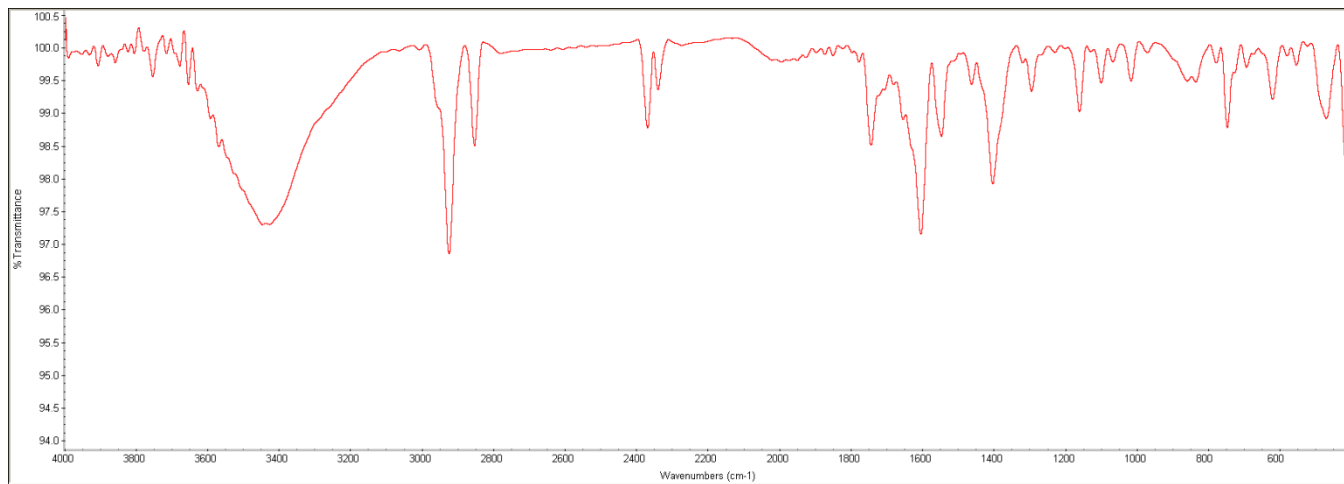
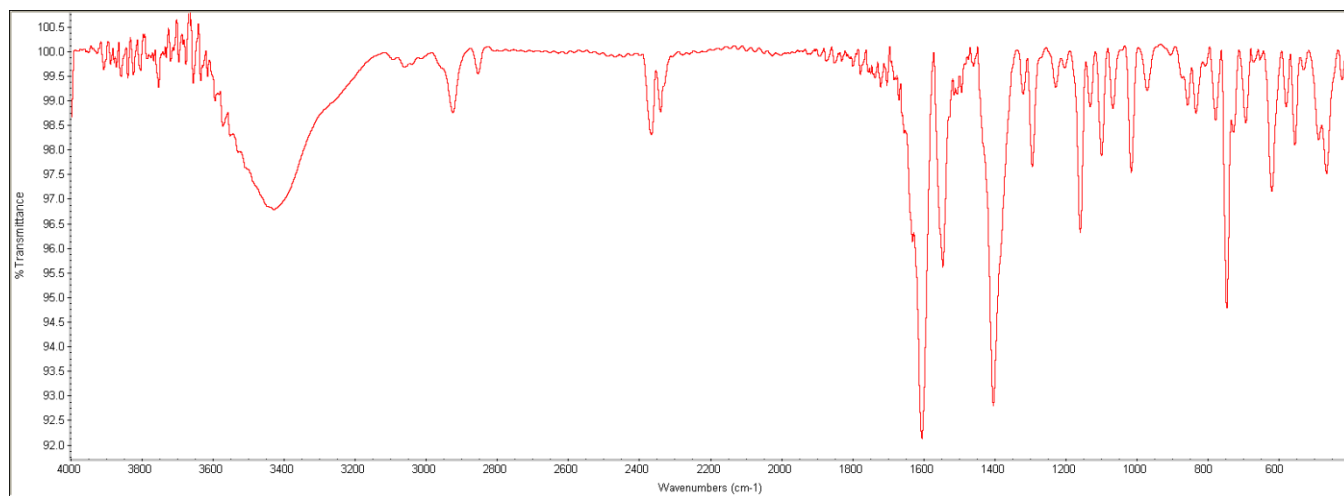


Fig. S12 ¹H-NMR spectrum of **1** in DMSO-*d*₆ with a small drop of HNO₃ to dissolve the crystals. The humps around 4.5 ppm is due to the protonated water (*-DMA).



(a)



(b)

Fig. S13 IR spectra of (a) **1** and (b) **2**.